

Surface plasmon mediated Raman scattering in metal nanoparticles

G. Bachelier and A. Mlayah

Laboratoire de Physique des Solides, UMR 5477, IRSAMC, Université P. Sabatier, 118 Route de Narbonne,
31062 Toulouse Cedex 4, France

(Received 10 December 2003; revised manuscript received 24 February 2004; published 26 May 2004)

The Raman scattering due to confined acoustic vibrations in metal particles is studied theoretically. Various coupling mechanisms between the surface plasmon–polaritons and the confined vibrations are investigated. Their relative contribution to the light scattering is discussed. We found that two mechanisms play an important role: (i) modulation of the interband dielectric susceptibility via deformation potential due to pure radial vibrations and (ii) modulation of the surface polarization charges by quadripolar vibrations. The dependence of the Raman spectra on the nanoparticles size and size distribution and on the excitation energy is studied in connection with the nature of the excited plasmon-polariton states. We found a good agreement between calculated line shapes and relative intensities of the Raman bands and the experimental spectra reported in the literature.

DOI: 10.1103/PhysRevB.69.205408

PACS number(s): 78.30.Er, 63.22.+m, 73.22.Lp, 78.67.Bf

I. INTRODUCTION

Surface-enhanced Raman scattering¹ has been attracting much interest recently due to the discovery of single-molecule sensitivity.^{2,3} The key role of randomly distributed⁴ or fractal-like aggregates⁵ in the disorder induced localization of the surface plasmons is now well established. In their earlier work,⁶ Gersten *et al.* showed that resonance of the incident light with the plasmons of a rough metal surface leads to strong light scattering by confined acoustic vibrations. For an isolated spherical particle, the phonon density of states is discrete and the confined vibrations are expressed in term of vector spherical harmonics labeled (n, l, m) . They can be obtained from Lamb's theory⁷ applied to nanosized particles (i.e., with a radius much larger than the interatomic distance). Many published experimental works showed that the confined quadripolar vibrations ($n=1, l=2$) strongly come out in the Raman spectra of Au, Ag, and Cu nanoparticles for resonant excitation with the surface plasmon absorption band.^{6,8,9} In contrast, the pure radial vibrations ($l=0$) are not easily observable and were revealed only recently^{10,11} in the Raman spectra of metal particles with a narrow size distribution. On the other hand, time-resolved reflectivity measurements showed periodic intensity oscillations due to pure radial vibrations ($n=1, l=0$) only.¹² Up to now it is not clear why the quadripolar vibrations should dominate in Raman scattering and pure radial vibrations in time-resolved reflectivity. A complete understanding of the optical properties of a vibrating metal particle still lacks. In their earlier work, Gersten *et al.*¹³ proposed a model for Raman scattering from size and shape distributed metal particles. They considered coupling between the dipolar surface plasmons and the quadripolar vibrations due to modulation of the electron charge density (i.e., of the bulk plasmon frequency). Pure radial vibrations were not expected to produce a significant modulation which is apparently in agreement with the experimental observations. Nevertheless, no calculations of the relative contribution of quadripolar and radial vibrations have been reported up to now. In addition, comparison with other possible coupling mechanisms is needed

in order to identify the origin of the Raman scattering.

Moreover, Montagna and Dusi¹⁴ proposed a model for the Raman scattering by confined acoustic vibrations of small dielectric spheres. The light scattering was described using the dipole-induced-dipole and bond polarizability models which are suitable for nonresonant scattering in dielectric materials, but cannot apply to resonant light scattering in metals.

In this work, we investigate and compare different coupling mechanisms between the confined vibrations and the surface plasmons of metal particles. They can be classified into surface and volume mechanisms. The surface mechanisms involve changes of the particle surface, whereas the volume mechanisms are due to modulation of the material properties. The Raman scattering efficiency is derived and discussed for each of them. Calculations are presented for silver nanoparticles but apply to gold and copper as well. The dependence of the scattering efficiency on average size and size distribution is discussed in connection with the resonantly excited surface plasmons. The effects of the surrounding medium are not investigated here. They are expected to shift the plasmon resonances and the vibration frequencies.¹⁵ However, they should not affect the conclusions of the present work with respect to the plasmon-vibration coupling and related Raman scattering.

II. MODEL

A. Surface plasmon–polariton states

We use the dielectric confinement model to account for the optical properties of the metal particles.¹⁶ The electromagnetic fields inside and outside the particle are computed from Maxwell equations (i.e., including retardation effects) and using the usual surface boundary conditions: continuity of the normal component of the magnetic field and of the tangential component of the electric field. Contributions of both intraband and interband transitions were taken into account in the frequency-dependent dielectric response of the metal particle. We use the size dependent dielectric susceptibility given by

$$\chi(\omega, R) = -\frac{\omega_p^2}{\omega^2 + i\omega\gamma(\omega, R)} + \chi^{ib}(\omega), \quad (1)$$

where ω_p is the bare plasmon frequency of bulk silver and $\gamma(\omega, R) = \gamma_o + gs(\omega)v_F/R$ the effective Drude damping which accounts for the electron scattering by the nanoparticle surface;¹⁷ v_F is the Fermi velocity and R the nanoparticle radius. $gs(\omega)$ is obtained from a quantum treatment of the electron-surface interaction. $\chi^{ib}(\omega)$ is the interband dielectric function due to electronic transitions from the $4d$ valence band to the $5s$ conduction band.¹⁸ As shown by Hovel *et al.*,¹⁹ $\chi^{ib}(\omega)$ does not change with particle size for $R > 1$ nm. Then $\chi^{ib}(\omega)$ was taken from the data reported for bulk silver in Ref. 20.

Solutions of Maxwell equations are obtained at all frequencies (continuous density of states). Hence, the electromagnetic field and polarization vectors are labeled $\mathbf{E}_{\omega, L, M}$ and $\mathbf{P}_{\omega, L, M}$, respectively; ω being the eigenfrequency and (L, M) the usual integer numbers associated with the spherical harmonic functions. The amplitude of the electromagnetic field inside the metal particle reaches a maximum for discrete frequencies ω_L known as the surface plasmon-polariton (SPP) resonances or as Mie's resonances.²¹ For spherical particles, ω_L is $(2L+1)$ -fold degenerate.

The lifetime of the SPP states is strongly reduced due to

Landau damping (i.e., to decay into electron hole pairs). From Fermi's golden rule one obtains the decay rate²²

$$\Gamma_{\omega, L}(R) = \Gamma_i + 2\pi \sum_{e, e'} |\langle e' | H_{\omega, L} | e \rangle|^2 \delta(\hbar\omega + \epsilon_e - \epsilon_{e'}), \quad (2)$$

where e and e' are individual electronic states and $H_{\omega, L}$ their interaction Hamiltonian with the SPP states ω, L . Γ_i is given by the bulk material properties. As discussed by Hovel *et al.*,¹⁹ Γ_i turns to be the Drude damping γ_0 [Eq. (1)] in the case of free-electron metals. Using Eq. (2) one recovers the well-known $1/R$ dependence.²² Moreover, $\Gamma_{\omega, L}(R)$ increases as the squared amplitude of the inner electric field associated with the SPP state (ω, L, M) . Hence, for nanoparticles one expects overdamping of the SPP resonant states with $L > 1$ due to their fast decay into electron-hole pairs.²⁴

B. Raman scattering

For the calculation of the Raman spectra, we assume a three-step scattering process²³ in which a SPP state (ω, L, M) is excited by the incoming photon and decays into another SPP state (ω', L', M') , via emission or absorption of confined (n, l, m) vibration; finally a scattered photon is emitted. For the Stokes process, the Raman scattering amplitude is given by

$$\begin{aligned} & -2i\pi\delta(\hbar\omega_s + \hbar\omega_{n, l} - \hbar\omega_i) \times \langle n_s + 1, n_{\omega', L', M'} | H_{ph-SPP} | n_s, n_{\omega', L', M'} + 1 \rangle \times \langle n_{\omega, L, M}, n_{\omega', L', M'} + 1, n_{n, l, m} \\ & + 1 | H_{vib-SPP} | n_{\omega, L, M} + 1, n_{\omega', L', M'}, n_{n, l, m} \rangle \times \frac{\langle n_i - 1, n_{\omega, L, M} + 1 | H_{ph-SPP} | n_i, n_{\omega, L, M} \rangle}{(\hbar\omega_s - \hbar\omega' + i\Gamma_{\omega', L'}) (\hbar\omega + i\Gamma_{\omega, L} - \hbar\omega_i)}, \end{aligned} \quad (3)$$

where n_i , n_s , $n_{\omega, L, M}$, and $n_{n, l, m}$ are, respectively, occupation numbers of incoming and outgoing photons, surface plasmon-polaritons (ω, L, M) , and confined vibrations (n, l, m) . $\Gamma_{\omega, L}$ is given by Eq. (2). H_{ph-SPP} and $H_{vib-SPP}$ correspond to the photon-SPP and confined vibration-SPP interaction Hamiltonians.

We assume dipolar interaction between the SPP states and the incoming or outgoing photons. Because spherical symmetry is preserved at the absorption or emission steps of the confined vibrations, conservation of the angular momentum should be fulfilled. This implies the following selection rules:

$$|L - L'| \leq l \leq L + L', \quad (4a)$$

$$L + L' + l \quad \text{even}, \quad (4b)$$

$$M' - M = \pm m. \quad (4c)$$

On the other hand, there is no restriction on the values of L and L' since the spherical symmetry is broken at the photon absorption and emission steps (interaction between plane waves and spherical harmonics). However, in the particular case of nanoparticles we consider only dipolar SPP states

(i.e., $L = L' = 1$) as discussed above. Thus, according to selection rules (4a) and (4b), only pure radial ($l=0$) and quadrupolar ($l=2$) vibrations could be observed by Raman scattering from spherical and noninteracting nanoparticles. This has been already pointed out by Duval²⁵ using group symmetry arguments. In the three-step light scattering process, it is the symmetry of the intermediate SPP state which determines the symmetry of the Raman active modes. Further considerations on the interaction between dipolar SPP states and vibrations can lead to additional selection rules or at least determine the relative contribution of the quadrupolar and the pure radial vibrations.

We now consider dipolar interaction between SPP states. Without particle vibrations, this interaction does not exist since the SPP form a set of orthogonal eigenstates. As the metal particle vibrates, so will the SPP polarization vector and then transitions between SPP states will take place.

Then the interaction matrix elements between confined (n, l, m) vibrations and those dipolar SPP states read

$$H_{vib-SPP} = - \int_{particle} \mathbf{E}_{\omega', L', M'} \cdot \delta_{n, l, m} \mathbf{P}_{\omega, L, M} dV, \quad (5)$$

where $\delta_{n,l,m}\mathbf{P}_{\omega,L,M}$ is the polarization modulation of the SSP state (ω,L,M) induced by the confined vibrations (n,l,m) . $\mathbf{E}_{\omega',L',M'}$ is the electric field associated with the final (ω',L',M') SPP state. For nanoparticles, only dipolar SPP states ($L=L'=1$) play an important role. The integral in Eq. (5) runs over the particle volume only because there is no polarization outside the metal particle (i.e., in vacuum). In order to calculate the Raman spectra one has to specify $\delta_{n,l,m}\mathbf{P}_{\omega,L,M}$.

C. Volume mechanisms

Let us start with the coupling between confined vibrations and SPP states due to what we named volume mechanisms. By volume mechanisms we mean modulation of the dielectric response independently from the surface motion. This concerns modulation of the bulk metal dielectric response due to changes of the material electronic properties. For instance, deformation potential (DP) interaction²⁶ between the lattice vibrations and the confined electronic states leads to modulation of the metal dielectric susceptibility (and hence of the SPP's polarization vectors).²⁷ In principle, both intraband and interband terms of the dielectric response can be modulated via DP interaction. However, because the single particle intraband excitations fall in the infrared range, the effect of their interaction with lattice vibrations on the collective intraband response is negligible in the visible range.²⁷ In other words, the bare plasmon frequency ω_p is not affected by lattice vibrations. On the contrary, electronic interband excitations fall in the UV range and lead to a strong screening effect of the bare plasmon. As a matter of fact, for bulk silver the bare plasmon energy is about 9 eV whereas the plasmon absorption band is observed around 3 eV. We have calculated the change of the interband dielectric susceptibility of silver due to DP interaction of the interband excitations with lattice vibrations. Since the interband susceptibility is independent of the particle size, quantum confinement effects on electronic states were neglected. In order to compute the overall change of $\chi^{ib}(\omega)$ one has to sum the contributions of transitions involving initial and final states from the whole Brillouin zone, the value of the DP energy depending on the considered states. We assume an average value $D^{e-ph} = -1.55$ eV intermediate between the values obtained for zone center (Γ point) and for zone edge (L point) states.²⁸ Hence, the modulation $\delta_{n,l,m}\mathbf{P}_{\omega,L,M}$ of the SPP polarization reads

$$\delta_{n,l,m}\mathbf{P}_{\omega,L,M} = \varepsilon_0 \chi^{inter}(\omega) \left(\frac{D^{e-ph}}{\hbar\omega - \hbar\Omega^{ib}} \nabla \cdot \mathbf{D}_{n,l,m} \right) \mathbf{E}_{\omega,L,M}. \quad (6)$$

In this equation, confinement effects of the lattice vibrations appear in the divergence of the displacement field $\nabla \cdot \mathbf{D}_{n,l,m}$. It is worthwhile to mention that Eq. (6) is valid for bulk as well. The only difference with the nanoparticles is the displacement field $\mathbf{D}_{n,l,m}$ which introduces the confinement of the lattice vibrations. In other words the value of D^{e-ph} itself is independent of the nanoparticle surface (or

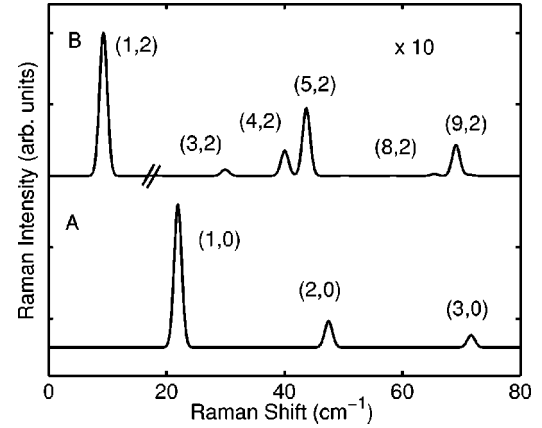


FIG. 1. Normalized Raman spectra of silver nanoparticles calculated with $R=2.5$ nm for resonant excitation with SPP state at 2.5 eV. Spectra correspond to the coupling via (A) deformation potential and (B) surface modulation mechanisms. The frequency range 16–80 cm^{-1} is shown with 10 \times magnification in spectrum (B). The linewidths result from convolution by a Lorentzian function.

radius). In that sense the DP coupling mechanism can be classified as a volume mechanism.

By making Eq. (6) into Eq. (5), and using the three-step light scattering process [Eq. (3)], we are able to calculate the Raman spectra due to DP coupling between confined vibrations and SPP states. As shown in Fig. 1, the Raman scattering (spectrum A) is dominated by the pure radial vibrations ($l=0$). The first three frequencies were found at 21.9 cm^{-1} , 47.5 cm^{-1} , and 71.6 cm^{-1} for $R=2.5$ nm. The intensity ratios between harmonics in spectrum A of Fig. 1 do not depend on the excitation energy since the electromagnetic field distribution inside the nanoparticle is uniform whatever the energy of the dipolar SPP state is. Quadripolar vibrations ($l=2$) are not forbidden since they satisfy selection rules (4a) and (4b). However, their Raman efficiency is here several orders of magnitude smaller than that of the pure radial vibrations.²⁹ Vallée *et al.* suggested that modulation of the interband susceptibility due to the confined vibrations could be responsible for the oscillation observed in the time-resolved reflectivity of metal nanoparticles.¹² From the oscillations period they identified pure radial vibrations ($n=1, l=0$). Quadripolar vibrations were not revealed. Portales *et al.*¹⁰ suggested that the same modulation is at the origin of the Raman scattering by pure radial vibrations ($l=0$). This is in agreement with our calculations. Indeed, for the DP mechanism, we found that modulation of the interband susceptibility by quadripolar vibrations ($n=1, l=2$) is one order of magnitude smaller than the one due to pure radial vibrations ($n=1, l=0$). This arises from the weak displacement field gradient associated with quadripolar vibrations. Moreover, it is clear that the DP mechanism cannot explain the intense lower frequency peak observed in the Raman spectra and ascribed to the fundamental quadripolar vibrations ($n=1, l=2$).^{9–11,13}

D. Surface mechanisms

The surface coupling mechanisms involve changes of the particle radius or shape. First, Gersten *et al.*¹³ proposed a

modulation of the bare plasmon frequency ω_p due to electron density oscillations with the particle volume. In fact, one can see in Eq. (1) that the size dependence of the intraband dielectric susceptibility arises from the Drude damping parameter only. For a silver particle with 3 nm radius excited at 3 eV (i.e., close to the dipolar SPP resonance) one obtains $g_s(\omega, R)v_F/R = 220$ meV.¹⁷ This term is more than one order of magnitude smaller than the excitation energy. So, in terms of relative changes, the effects of particle vibrations on Drude damping, and consequently on the intraband dielectric response, are very weak.²⁷ Second, in the frame of the dielectric confinement model, the energies of SPP resonances are determined by the electromagnetic boundary conditions at the nanoparticle surface. Strictly speaking, they should be sensitive to oscillations of the particle radius. The dependence of the resonant SPP eigenfrequency on the particle size arises from the retardation effects which are negligible for nanosized particles (particle radius very small in comparison with the visible optical wavelengths). Hence, this coupling mechanism is also very weak. It is worthwhile to mention that all surface coupling mechanisms discussed above involve only pure radial vibrations ($l=0$) because they are associated with changes of the particle volume. Therefore, they cannot explain the lower-frequency Raman peak assigned to quadrupolar vibrations. Moreover, compared to the DP coupling mechanism, the surface mechanisms discussed above are several order of magnitudes less efficient.

The change of the particle shape can also lead to a modulation of the SPP polarization vectors. Indeed, the polarization vectors of the SPP states are associated with a distribution of polarization charges at the nanoparticle surface given by $\mathbf{P}_{\omega, L, M} \cdot \mathbf{n}$, \mathbf{n} being the normal to the surface. Therefore, when the particle oscillates, in the (n, l, m) vibration mode, its orientation varies by $(\delta_{n, l, m} \mathbf{n})$; so the polarization charges are redistributed with respect to the static situation according to $\delta_{n, l, m} \sigma_{\omega, L, M} = \mathbf{P}_{\omega, L, M} \cdot \delta_{n, l, m} \mathbf{n}$. This is what we call surface orientation (SO) coupling mechanism. In order to evaluate the modulation $\delta_{n, l, m} \mathbf{P}_{\omega, L, M}$ of the SPP polarization, we expand $\delta_{n, l, m} \sigma_{\omega, L, M}$ on the basis of the surface polarization charges $\sigma_{\omega, L', M'}$ of the motionless particle,

$$\delta_{n, l, m} \sigma_{\omega, L, M} = \sum_{L', M'} \frac{\int \sigma_{\omega, L', M'} \delta_{n, l, m} \sigma_{\omega, L, M} \cdot dS}{\int \sigma_{\omega, L', M'}^2 \cdot dS} \sigma_{\omega, L', M'}. \quad (7)$$

By making $\sigma_{\omega, L', M'} = \mathbf{P}_{\omega, L', M'} \cdot \mathbf{n}$ in Eq. (7) one can rewrite $\delta_{n, l, m} \sigma_{\omega, L, M}$ as $\delta_{n, l, m} \mathbf{P}_{\omega, L, M} \cdot \mathbf{n}$ with

$$\delta_{n, l, m} \mathbf{P}_{\omega, L, M} = \varepsilon_0 \chi(\omega) \sum_{L', M'} \frac{\int \sigma_{\omega, L', M'} \delta_{n, l, m} \sigma_{\omega, L, M} \cdot dS}{\int \sigma_{\omega, L', M'}^2 \cdot dS} \times \mathbf{E}_{\omega, L', M'}. \quad (8)$$

In the SO coupling mechanism, only quadrupolar spheroidal vibrations contribute to Raman scattering. Pure trans-

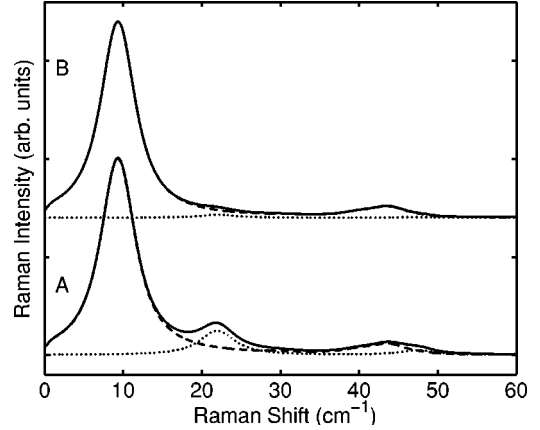


FIG. 2. Normalized Raman spectra of silver nanoparticles calculated with $R=2.5$ nm for resonant excitation with SPP states at (A) 2.5 eV and (B) 2 eV. The contributions of the deformation potentials and surface orientation mechanisms are shown by dotted and dashed lines, respectively. The total scattered intensity is shown as bold lines. The linewidths result from the convolution by a Lorentzian function (finite experimental resolution) and from the size-dependent vibrational lifetime.

verse and pure radial vibrations are not active because such modes do not change the shape of the particle surface. Moreover, this mechanism is sensitive to the displacement field at the particle surface only. Therefore, the intensity ratio between harmonics [spectrum B of Fig. 1] strongly differ from the one calculated for DP coupling [spectrum A]. The first three quadrupolar vibrations were found at 9.3 cm^{-1} , 18.1 cm^{-1} , and 30 cm^{-1} for 2.5 nm particle radius. The most intense contribution from the harmonics is due to the quadrupolar ($n=5, l=2$) modes. The corresponding Raman peak [spectrum B] is 20 times weaker than that of the fundamental vibrations ($n=1, l=2$). This explains why only the fundamental quadrupolar vibration modes were observed experimentally for nanoparticles ensembles with large size dispersion.^{6,8,9}

III. RESULTS AND DISCUSSION

A. Origin of the Raman bands

Calculation of the Raman scattering efficiencies allows to estimate the contributions of different coupling mechanisms and hence identify the origin of the low-frequency Raman bands. The spectra calculated, assuming both DP and SO coupling mechanisms, are shown in Fig. 2 for an isolated spherical particle with 2.5 nm radius. Calculations were performed for resonant excitation of the SPP states at 2 eV and 2.5 eV, close to the dipolar SPP resonance observed in Ref. 11. We use a size-dependent homogeneous broadening of the confined vibrations given by¹² $\Gamma_{n, l}(R) = 2\pi c_l / (\tau_{n, l} R)$, c_l being the longitudinal sound velocity. $\tau_{n, l}$ is a measure of how fast the vibrational excitations fade away.³⁰ We found that $\tau_{n, l} \approx 10$ for all modes give a reasonable agreement between the calculated and measured spectra reported in the literature.^{10,11} In comparison with Fig. 1, only three bands

appear in the simulated spectra (A) of Fig. 2. The intense lower-frequency peak is due to scattering by the fundamental quadrupolar vibrations ($n=1, l=2$) coupled to the dipolar SPP states via SO mechanism. The weaker band, around 22 cm^{-1} , is associated with the fundamental radial mode ($n=1, l=0$). Its coupling to the dipolar SPP states occurs via DP mechanism. The higher-frequency band around 45 cm^{-1} has contributions from quadrupolar ($n=4$ and $5, l=2$) and pure radial ($n=2, l=0$) harmonics. The agreement with the measured Raman spectra reported in Ref. 11 is remarkable. In particular, the relative intensities of the Raman bands are well reproduced.

We would like to emphasize that the calculated intensities are directly determined by Eqs. (6) and (8). Only two physical quantities could be viewed as adjustable parameters: the averaged deformation potential D^{e-ph} and the parameter $\tau_{n,l}$ related to the vibration lifetime, which acts as an homogeneous broadening of the Raman lines. We used the same value of $\tau_{n,l}$ for all vibration modes. Hence, the relative intensities of the calculated bands do not depend on $\tau_{n,l}$. The best agreement with the results of Ref. 11 was obtained for $\tau_{n,l}=10$. This value is three times larger than that obtained by Del Fatti *et al.*¹² for particles embedded in glass matrix. This indicates a weaker coupling between the confined vibrations and the surrounding medium as expected for the particles studied in Ref. 11 which were coated with thiol chains. The value $\tau_{n,l}=10$ is in good agreement with the one obtained by Voisin *et al.*³¹ on silver particles in colloidal suspension. Concerning the averaged deformation potential, we did not try to adjust D^{e-ph} . Strictly speaking, its value should be calculated from the electronic properties of the overall Brillouin zone as discussed above. Since the electronic states at the Fermi level involve mainly the zone center and the (L -point) zone edge, we used an average potential extracted from Ref. 28. This value is, of course, material dependent and can also be modified by quantum confinement effects not taken into account.

An important issue of our simulations is that all Raman bands^{10,11} do not originate from the same scattering mechanism and can be accounted for without invoking any ellipsoidal distortion of the particle shape, although this may play an important role, as already suggested by Portales *et al.*¹⁰ The dependence of the Raman scattering on incident and scattered photon polarizations can be used to ascertain the origin of the observed bands: since the scattering due to pure radial vibrations is totally polarized, the band around 22 cm^{-1} should disappear in crossed polarizations, whereas the band around 45 cm^{-1} is expected to shift toward lower frequencies due to extinction of the vibration harmonic ($n=2, l=0$). Obviously, these predicted selection rules should be reconsidered in the case of interacting particles or non-spherical particles.

It is interesting to notice that the DP mechanism involves modulation of the dielectric susceptibility and hence pure radial vibrations can be detected in the oscillatory part of the time-resolved reflectivity. In the SO mechanism, it is the SPP polarization vector and not the dielectric susceptibility which is modulated by the particle vibrations. The modulation $\delta_{n,l,m} \mathbf{P}_{\omega,L,M}$ given by Eq. (8) arises from the redistribution

of the surface polarization charges. Hence, the reflectivity is not modulated and quadrupolar vibrations could not be observed in time-resolved reflectivity measurements.¹²

The different nature of the DP and SO coupling mechanisms leads to different behaviors of the Raman scattering efficiency with respect to excitation energy. Indeed, according to Eq. (6) the DP mechanism involves modulation of the interband susceptibility, only. For the SO mechanism, the modulation of the SPP polarization vectors is proportional to the overall dielectric susceptibility [Eq. (8)]. Therefore, the relative contribution of both mechanisms is expected to change with excitation energy, as shown in Fig. 2. At low excitation energy (spectrum B), the interband susceptibility is rather small with respect to the overall dielectric susceptibility. Then, mainly quadrupolar vibrations do contribute to the low-frequency Raman spectra. On the contrary, for excitation close to the SPP resonance (spectrum A), the Raman scattering due to pure radial modes ($l=0$) comes out since the interband susceptibility has a larger contribution. Unlike silver, for which interband transitions fall in the UV domain, gold has a strong interband susceptibility in the visible range. So one expects that Raman scattering by pure radial modes ($l=0$) is more easily observed for gold nanoparticles than for silver. This has been already verified experimentally by Portales *et al.*¹⁰

B. Effects of size distribution

The spatial distribution of the electric field and polarization associated with the SPP states strongly depends on the particle size, but also on the considered state. The SPP states are intermediate states for the Raman scattering process. Therefore, the dependence of the low-frequency Raman bands on the particle size is not only due to the well-known $1/R$ frequency variation of the confined vibration modes. It also reflects the change of the interaction matrix elements, i.e., absolute Raman intensities, line shapes, and frequencies.

For excitation close to the dipolar SPP resonance ($\omega_{ex} \approx \omega_{L=1}$), the intensity of Rayleigh scattering was found to be proportional to V^2 (V being the particle volume).³² For Raman scattering, the additional interaction step between confined vibrations and SPP states must be taken into account. We found that the vibration-SPP coupling strength varies as $1/R^4$ for both DP and SO mechanisms. The Raman efficiency is thus proportional to $V^2/R^4 = R^2$ as already pointed out by Duval *et al.*⁹ for crystallized particles. Hence, the frequencies of the Raman bands do not coincide with the vibration frequencies calculated for the average size of the nanoparticles. This is shown in Fig. 3 for the lowest-frequency band, associated with confined quadrupolar vibrations. For small size dispersion (less than 10%), the shift is one order of magnitude smaller than typical spectrometer resolution (about 2 cm^{-1}). In contrast, with 40% size dispersion, the contribution of large particles dominates, leading so to a noticeable down shift of the Raman bands.

As shown in Fig. 3, the sensitivity of the Raman scattering to size dispersion of the nanoparticles depends on the excitation energy. Indeed, for nanoparticles excited well below the dipolar SPP resonance ($\omega_{ex} < \omega_{L=1}$), the down shift

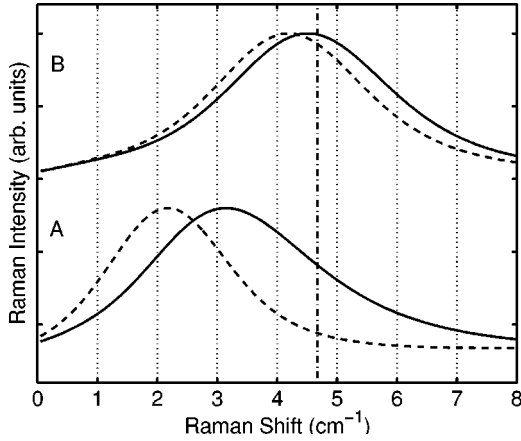


FIG. 3. Normalized Raman spectra of silver nanoparticles calculated with an average radius $R=5$ nm for excitation energy at 3 eV (bold lines) and 2 eV (dashed lines). The simulations were performed with 10% (A) and 40% (B) size dispersion and assuming a size dependent vibration lifetime. The vertical dashed-dotted line corresponds to the frequency of the fundamental quadrupolar mode calculated for $R=5$ nm.

of the Raman bands with size dispersion is very pronounced. A close inspection of the interaction matrix elements reveals that this very sharp dependence arises from the nature of the intermediate SPP states: for $\omega_{ex} < \omega_{L=1}$ the excited SPP states have electric fields weakly confined inside the metal particle and are therefore rather independent of the particle radius. Then, the interaction matrix elements for the photons-SPP and vibrations-SPP interactions increase as the particle volume. Hence, the Raman scattering efficiency was found to be proportional to V^6/R^4 . This sharp dependence is responsible for the different shifts obtained for the resonant and nonresonant situations shown in Fig. 3. For $\omega_{ex} > \omega_{L=1}$, the situation is similar (weak confinement effect of the electric fields associated with SPP). However, the resonant contribution of interband transitions to the Raman scattering should be taken into account. In that case one has to consider electron-hole pairs as possible intermediate states of the scattering process. This is beyond the scope of the present work.

The intensities shown in Fig. 3 were normalized using appropriate scaling factors. In fact, for excitation away from the SPP resonance (at 2 eV) we found that the scattering amplitude is much weaker than that calculated for excitation close to resonance (3 eV). This is partly due to the weakening of the electric-field amplitude [in the interaction matrix elements of Eq. (3)] inside the metal particle. The out of resonance/in resonance intensity ratio depends also on the SPP damping [see Eq. (3)]. We used the plasmon damping given by Eq. (2) in our calculations.²² Since the Landau damping is proportional to the scattered amplitude of the inner field, it is expected to be very small for nonresonant SPP states. Hence for these states only remains the contribution Γ_i extracted from the bulk material properties. We used $\Gamma_i = 0.14$ eV given in Ref. 20.

Since the SO and DP coupling mechanisms have the same dependence on the particle size, one expects the same frequency shift with excitation energy of the Raman bands associated with quadrupolar and pure radial vibrations. However, as shown in Fig. 2 (spectrum B), emission of pure radial vibrations is weak for excitation below the dipolar SPP resonance. This means that nonresonant SPP states contribute only little to the Raman scattering by pure radial vibrations. For this reason, we found only a small frequency shift with excitation energy for the Raman bands due to pure radial vibrations. This is in agreement with the experimental data reported by Portales *et al.*¹⁰

IV. CONCLUSION

We have performed calculations of the Raman scattering efficiency of silver nanoparticles excited close to resonance with the dipolar surface plasmon-polariton resonance. We assumed a three-step scattering process and studied the interaction between confined acoustic vibrations and surface plasmon-polariton states. Several coupling mechanisms were considered. Our main findings can be summarized as follows.

(i) The origin of the lower-frequency intense peak, observed in the Raman spectra of metal particles and ascribed to the fundamental mode of the confined quadrupolar vibrations, has been identified: it is due to modulation of the dipolar SPP polarization by the change in the surface orientation as the nanoparticle oscillates. This mechanism involves quadrupolar vibrations only. Pure radial vibrations are not active since the surface orientation is unaffected by such modes.

(ii) The higher-frequency bands recently revealed in the Raman spectra of metal particles with narrow size distribution are due to combinations of fundamental and overtones of pure radial and quadrupolar vibrations. Scattering by pure radial vibrations is due to modulation of the interband susceptibility and SPP polarization vectors via deformation potential mechanism. The calculated Raman line shapes and intensity ratios are in good agreement with the experimental data published in the literature.

(iii) While in Raman scattering both SO and DP mechanisms manifest, only DP mechanism is relevant for time-resolved reflectivity. That is why only pure radial vibrations can be observed as periodic oscillations of the time-resolved reflectivity. The detailed analysis of the Raman scattering requires identification of the intermediate resonant states and their various coupling mechanisms to the vibrations. Our calculations were performed for the simplest case of spherical and isolated particles surrounded by vacuum. Nevertheless, they shed light on the origin of the low-frequency Raman scattering in metal nanoparticles. The effects of interaction between nanoparticles, nonspherical shapes, and surrounding medium should affect the frequencies, line shapes, and selection rules of the Raman bands.

- ¹M. Moscovits, Rev. Mod. Phys. **57**, 783 (1985).
- ²K. Kneipp, Y. Wang, H. Kneipp, L.T. Perelman, I. Itzkan, R.R. Dasari, and M.S. Feld, Phys. Rev. Lett. **78**, 1667 (1997).
- ³H. Xu, E.J. Bjerneld, M. Kall, and L. Borjesson, Phys. Rev. Lett. **83**, 4357 (1999).
- ⁴K. Arya, Z.B. Su, and J.L. Birman, Phys. Rev. Lett. **54**, 1559 (1985).
- ⁵M.I. Stockman, V.M. Shalaev, M. Moskovits, R. Botet, and T.F. George, Phys. Rev. B **46**, 2821 (1992).
- ⁶D.A. Weitz, T.J. Gramila, A.Z. Genack, and J.I. Gersten, Phys. Rev. Lett. **45**, 355 (1980).
- ⁷A. E. H. Love, *A Treatise on the Mathematical Theory of Elasticity* (Dover, New York, 1944).
- ⁸M. Fujii, T. Nagareda, S. Hayashi, and K. Yamamoto, Phys. Rev. B **44**, 6243 (1991).
- ⁹B. Palpant, H. Portales, L. Saviot, J. Lerme, B. Prevel, M. Pelletier, E. Duval, A. Perez, and M. Broyer, Phys. Rev. B **60**, 17 107 (1999); E. Duval, H. Portales, L. Saviot, M. Fujii, K. Sumitomo, and S. Hayashi, *ibid.* **63**, 075405 (2001).
- ¹⁰H. Portales, L. Saviot, E. Duval, M. Fujii, S. Hayashi, N. Del Fatti, and F. Vallee, J. Chem. Phys. **115**, 3444 (2001).
- ¹¹A. Courty, I. Lisiecki, and M.P. Pileni, J. Chem. Phys. **116**, 8074 (2002).
- ¹²N. Del Fatti, C. Voisin, F. Chevy, F. Vallée, and C. Flytzanis, J. Chem. Phys. **110**, 11 484 (1999).
- ¹³J.I. Gersten, D.A. Weitz, T.J. Gramila, and A.Z. Genack, Phys. Rev. B **22**, 4562 (1980).
- ¹⁴M. Montagna and R. Dusi, Phys. Rev. B **52**, 10 080 (1995).
- ¹⁵N.N. Ovsyuk and V.N. Novikov, Phys. Rev. B **53**, 3113 (1996).
- ¹⁶K. Arya and R. Zeyher, in *Lighth Scattering in Solids IV*, edited by M. Cardona and G. Gntherodt (Springer-Verlag, Berlin, 1984).
- ¹⁷F. Hache, D. Richard, and C. Flytzanis, J. Opt. Soc. Am. B **3**, 1647 (1986).
- ¹⁸J. Lindhard, K. Dan. Vidensk. Selsk. Mat.-Fys. Medd. **28**, 8 (1954).
- ¹⁹H. Hovel, S. Fritz, A. Hilger, U. Kreibig, and M. Vollmer, Phys. Rev. B **48**, 18 178 (1993).
- ²⁰P.B. Johnson and R.W. Christy, Phys. Rev. B **6**, 4370 (1972).
- ²¹G. Mie, Ann. Phys. (Leipzig) **25**, 377 (1908).
- ²²R.A. Molina, D. Weinmann, and R.A. Jalabert, Phys. Rev. B **65**, 155427 (2002).
- ²³P.Y. Yu and M. Cardona, *Fundamentals of Semiconductors* (Springer-Verlag, Berlin, 1999).
- ²⁴The electromagnetic field amplitude associated with the resonant SPP states ω_L is proportional to the Bessel function $\eta_L(k_{ex,L}R)$ where $k_{ex,L}$ is the wave vector outside the nanoparticle, i.e., to $(\lambda_{ex,L}/R)^L$ for nanometer-sized particles ($\lambda_{ex,L} \gg R$).
- ²⁵E. Duval, Phys. Rev. B **46**, 5795 (1992).
- ²⁶J. Bardeen and W. Shockley, Phys. Rev. **80**, 72 (1950).
- ²⁷N. Del Fatti, C. Voisin, M. Achermann, S. Tzortzakakis, D. Christofilos, and F. Vallee, Phys. Rev. B **61**, 16 956 (2000).
- ²⁸H. Tups, A. Otto, and K. Syassen, Phys. Rev. B **29**, 5458 (1984).
- ²⁹For excitation of the resonant SPP states, the Raman intensity ratio between the quadrupolar and the radial vibrational modes is proportional to $(k_{in,L}R)$ (Ref. 4), where $k_{in,L}$ is the wave vector inside the nanoparticle. Then, for $k_{in,L}R \ll 1$, the contribution of the quadrupolar vibrational modes ($l=2$) to the Raman scattering is very weak.
- ³⁰This is the only place where the effect of the surrounding medium was taken into account.
- ³¹C. Voisin, Ph.D. thesis, Paris XI Orsay University, 2001.
- ³²A.J. Cox, A.J. DeWeerd, and J. Linden, Am. J. Phys. **70**, 620 (2002).